Mon. Not. R. Astron. Soc. **000**, 1–?? (2007) Printed 5 September 2007 (MN LATEX style file v2.2)

Environments of $z > 5$ quasars: searching for protoclusters at submillimetre wavelengths

R. S. Priddey,[1] R. J. Ivison[2,3] and K. G. Isaak[4]

[1] *Centre for Astrophysics Research, Science and Technology Research Centre, University of Hertfordshire, College Lane, Herts AL10 9AB*
[2] *UK Astronomy Technology Centre, Royal Observatory, Blackford Hill, Edinburgh EH9 3HJ*
[3] *Institute for Astronomy, University of Edinburgh, Blackford Hill, Edinburgh EH9 3HJ*
[4] *School of Physics & Astronomy, Cardiff University, The Parade, Cardiff CF24 3AA*

DRAFT DATED: 5 SEPTEMBER 2007

ABSTRACT

The most massive haloes at high redshift are expected, according to hierarchical cosmologies, to reside in the most biased density fields. If powerful active galactic nuclei (AGN) are expected to exist anywhere in the early Universe ($z > 5$), it is within these massive haloes. The most luminous of these AGN, powered by supermassive black holes (SMBHs) $\sim 10^9\,\mathrm{M}_\odot$, thereby present an opportunity to test models of galaxy formation. Here, we present submillimetre (submm) continuum images of the fields of three luminous quasars at $z > 5$, obtained at 850 and 450 μm using the Submm Common-User Bolometer Array (SCUBA) on the James Clerk Maxwell Telescope (JCMT). N-body simulations predict that such quasars evolve to become the central dominant galaxies of massive clusters at $z = 0$, but at $z = 5 - 6$ they are actively forming stars and surrounded by a rich proto-filamentary structure of young galaxies. Our purpose in taking these images was to search for other luminous, star-forming galaxies in the vicinity of the signpost AGN and thus associated with such a protocluster. Two of the quasar host galaxies are luminous SMGs in their own right, implying star-formation rates (SFRs) $\sim 10^3\,\mathrm{M}_\odot\,\mathrm{yr}^{-1}$. Despite the coarse 850-μm beam of the JCMT, our images show evidence of extended emission on a scale of $\sim$100-kpc from at least one quasar – indicative of a partially resolved merger or a colossal host galaxy. In addition, at $>3\sigma$ significance we detect 12 (5) submm galaxies (SMGs) at 850 μm (450 μm) in the surrounding fields. Number counts of these SMGs are comparable with those detected in the fields of $z \sim 4$ radio galaxies, and both samples are systematically overabundant relative to blank-field submm surveys. Whilst the redshift-sensitive 850 μm/450 μm and 850 μm/1.4 GHz flux density ratios indicate that some of these SMGs are likely foreground objects, the counts suggest that many probably lie in the same large-scale structures as the quasars.

Key words:

1 INTRODUCTION

The search for $z > 5$ galaxies has taken on a new urgency in recent years. The epochal discovery of Gunn & Peterson (1965) absorption in the spectra of $z > 6$ quasars (Becker et al. 2001) suggests that reionisation was complete by $z = 6$. On the other hand, polarisation results from the *Wilkinson Microwave Anisotropy Probe* (*WMAP*) point to the onset to reionisation at $z \sim 12$ (Spergel et al. 2007). A primary goal of observational cosmology is, consequently, to locate and to characterise the galaxies (e.g. Bunker et al. 2004; Bouwens et al. 2006), quasars (e.g. Fan et al. 2006) and – via gamma-ray bursts – even individual stars (Jakobsson et al. 2006; Haislip et al. 2006) that existed during this period of cosmic phase transition, $\sim$0.4–1 Gyr after the Big Bang.

Although it is thought that the ultraviolet (UV) light from young stars, rather than AGN, provided the bulk of the ionizing radiation (Fan et al. 2006; Srbinovsky & Wyithe 2007), very high-redshift quasars are nevertheless important objects in their own right. SMBHs are found ubiquitously in the cores of nearby galaxies; studying their accretion-powered growth phase, during which they manifest themselves as high-redshift AGN, provides a window on the formation and evolution of the ancestors of present-day massive galaxies. The very existence of luminous AGN at redshifts above five imposes important constraints on processes governing the formation of massive galaxies, SMBHs and protoclusters in the early Universe. Their bolometric powers imply accretion onto SMBHs at a prodigious rate ($\sim 1\,\mathrm{M}_\odot\mathrm{yr}^{-1}$, assuming Eddington-limited accretion). Measurements based on the line width of Mg II indicate SMBH masses of $\sim 10^{9.5}\,\mathrm{M}_\odot$ (Willott et al. 2003), implying a host dark matter halo of mass $\sim 10^{12.5}$-$\mathrm{M}_\odot$ (Croom et al. 2005). Submm photometry of the host galaxies of

Table 1. Properties of target $z > 5$ quasars and their host galaxies.

Source Name	z	$M_{\rm B}$	R.A. (J2000)	Dec.	$S^{\rm phot}_{1250\mu{\rm m}}$ (mJy)	$S^{\rm phot}_{850\mu{\rm m}}$ (mJy)	$S^{\rm phot}_{450\mu{\rm m}}$ (mJy)	$S_{1.4{\rm GHz}}$ (μJy)
SDSS J0756+4104	5.09	−26.9	07 56 18.14	+41 04 08.6	5.5 ± 0.5	13.3 ± 2.1	14 ± 19	65 ± 15
SDSS J1030+0524	6.28	−27.7	10 30 27.10	+05 24 55.0	<3.4	1.3 ± 1.0	-21 ± 10	<61
SDSS J1044−0125	5.73	−28.0	10 44 33.04	−01 25 02.1	2.5 ± 0.55	6.1 ± 1.2	—	<79

$z > 5$ quasars reveal copious quantities of dust ($\sim 10^{8-9}\,{\rm M}_\odot$ – Priddey et al. 2003b; Robson et al. 2004) and CO emission lines imply $\sim 10^{10-11}\,{\rm M}_\odot$ of molecular gas (Walter et al. 2003, 2004). Both are indicative of strong star formation; indeed, a colossal starburst is required if the dust has been synthesised on the short timescale available ($\lesssim$1 Gyr since the Big Bang; $\lesssim$600 Myr since the onset of reionization).

The existence of massive, collapsed haloes at high redshift might appear to conflict with the prevailing hierarchical cold dark matter (CDM) model of structure formation, in which the initial density fluctuations have higher power on smaller scales. Using the Press–Schechter approximation, for example, Efstathiou & Rees (1988) predicted a marked decline in the number density of quasars at $z > 5$. To accommodate the growing sample of luminous AGN spectroscopically confirmed to lie at $z > 5$ within the CDM scheme, they are identified as corresponding to rare, high-σ peaks in the initial overdensity distribution. As such, they constitute excellent laboratories in which to test the predictions of structure-formation models operating *in extremis*. Specifically, high-σ haloes should be *biased* – more spatially correlated than the underlying mass – since neighbouring fluctuations sitting atop a low-amplitude, large-scale mode of the overdensity spectrum are boosted over the collapse threshold sooner (Kaiser 1984). The vicinity of a high-redshift, luminous AGN would thus be expected to contain an overabundance of massive, actively star-forming galaxies, the progenitor of a rich cluster at $z = 0$. More recently, the phenomenon of "downsizing" provides a framework in which galaxy formation at high redshift is completed earlier in more massive objects. Specifically, the semi-analytic "Anti-hierarchical Baryon Collapse" model of Granato et al. (2004) suggests an intimate evolutionary link between quasars and SMGs, feedback from the AGN playing an important role in regulating star formation in the host.

The submm waveband is an eminently appropriate place in which to search for structure, as traced by dusty, star-forming galaxies surrounding high-redshift AGN. This conjecture is supported by submm/mm imaging campaigns which have identified an excess of SMGs in fields centred on $z \sim 4$ radio galaxies (Ivison et al. 2000a; Stevens et al. 2003; De Breuck et al. 2004; Greve et al. 2007) and a $z \sim 2$ absorbed QSO (Stevens et al. 2004). In this paper, we extend this work to higher redshift, and expand upon our earlier photometric submm programmes (Isaak et al. 2002; Priddey et al. 2003a), obtaining very deep submm imaging of the fields of three $z > 5$ radio-quiet quasars.

Throughout, we assume cosmological parameters $\Omega_{\rm M} = 0.27$, $\Omega_\Lambda = 0.73$ and $H_0 = 71\,{\rm km\,s^{-1}\,Mpc^{-1}}$ (Spergel et al. 2007).

2 OBSERVATIONS AND DATA ANALYSIS

2.1 The sample

Three fields centred on quasars at $z > 5$ were selected for observation. The quasars were all discovered as part of the Sloan Digital Sky Survey (SDSS) by Fan et al. (2000, 2001) and Anderson et al. (2001). Their properties are listed in Table 1: all three are luminous at optical wavelengths (absolute B magnitudes in Table 1 are extrapolated from 1450Å continuum flux assuming a spectral index, -0.5), implying black hole masses of $\sim 10^{9.3-9.7}\,{\rm M}_\odot$, assuming a bolometric correction from the B band of 12 (Elvis et al. 1994) and Eddington-limited accretion. The sample was also designed to provide contrast in far-infrared luminosity, containing both the brightest member of the Priddey et al. (2003b) submm photometry sample (SDSS J0756+4104, $S_{850\mu{\rm m}} = 13.4\,{\rm mJy}$) and the deepest upper limit (SDSS J1030+0524, $S_{850\mu{\rm m}} < 2\,{\rm mJy}$).

2.2 Observations

Jiggle-map observations were made using the SCUBA bolometer array (Holland et al. 1999) on the 15-m JCMT over the period between 2001 Feb 28 and 2002 Mar 23. In each case the array was centred on the optical position of the quasar. Every 16 s the telescope was nodded in either right ascension or declination by 30 arcsec in an ON–OFF–OFF–ON sequence, with the secondary mirror chopping continually at $\sim$7 Hz between the ON and OFF positions. For SDSS J1044−0125, we nodded and chopped east-west (E–W) throughout. For SDSS J0756+4104 and SDSS J1030+0524 we nodded and chopped north-south (N–S) as the target rose and set, and E–W when the target was near transit. By adopting this latter strategy we ensured the chop direction was as close to azimuthal as possible and that the region within 30 arcsec of the outer bolometers was chopped onto the array; also, using several position angles reduced the chance of chopping one submm source systematically onto another.

Dynamic scheduling at JCMT ensured weather conditions were exceptionally good for our observations. The sky was stable and very transparent, with a median $\tau^{\rm zenith}_{225{\rm GHz}}$ of around 0.043 (often $<$0.04, never worse than 0.09). Flux calibration was determined by imaging CRL 618, Mars and Uranus and is accurate to 10 percent at 850 μm and 25 percent at 450 μm. A long imaging scan of 3C 345 was obtained, using the same observing strategy, to establish an accurate point spread function (PSF).

The total number of integrations/time expended on each field were: SDSS J0756+4104 (304 integrations; 38.9 ks); SDSS J1030+0524 (280 integrations; 35.8 ks); SDSS J1044−0125 (312 integrations; 39.9 ks).

In addition, we publish here for the first time a 250GHz on-off photometric observation of SDSS J1044−0125 obtained using the Max Planck Institut für Radioastronomie Millimetre BOlometer (MAMBO) array on the Institute de Radioastronomie Millimétrique (IRAM) 30-m telescope on Pico Veleta, Spain. The sky

opacity during the observations was in the range 0.164–0.260. Data were reduced using the GILDAS software package, yielding a 1.2-mm flux density 2.5 ± 0.6 mJy (4.5σ).

2.3 Data reduction

Data from SCUBA were reduced in a standard manner with the SURF package (Jenness & Lightfoot 1998), using modifications to the SETBOLWT and REBIN tasks developed for the survey of high-redshift radio galaxies by Ivison et al. (2000a) and Stevens et al. (2003), as described by Ivison (2006). Briefly, we created an astrometric grid of 1-arcsec^2 square pixels then determined accurately weighted and calibrated signal and noise measurements for each pixel, each measurement being wholly independent of values for its neighbouring pixels, with 13.4-arcsec FWHM resolution at 850 μm. These signal and noise values reflect the stream of data collected when bolometers are centred within the region of sky corresponding to a particular pixel. These unsmoothed images were used for source detection (see §2.4).

The submm images of each of the three quasar fields – 850-μm contours superposed on greyscale representations of the 450-μm data – are shown in Fig. 1, where we have smoothed with 6- and 3-arcsec FWHM Gaussians and the resulting 850- and 450-μm maps have typical noise levels of 1.5 and 7 mJy beam^{-1}. For comparison, the 5σ 850-μm confusion limit for the JCMT is ≈1–1.5 mJy, so we have reached close to the depth at which confusion is likely to begin posing problems.

2.4 Source detection

Source detection at 850 μm was accomplished using the algorithm described in detail by Scott et al. (2002), utilising the signal and noise maps and a PSF (measured for the blazar, 3C 345) to perform a simultaneous maximum-likelihood fit to all the potentially significant peaks in each map. Sources down to a significance level of $3\,\sigma$ are listed in Table 2.

Adopting a 3σ detection threshold, at 850 μm (450 μm) a total of 14 (7) sources are detected: 2 (1) QSOs and 12 (6) companions in the three fields, with flux densities between 4.4 (16) and 13.4 mJy (56 mJy). Five sources, including one QSO, are detected at both wavelengths (Table 2).

Discussing each of the fields in turn:

SDSS J0756+4104 (z = 5.09) was detected via photometry-mode (on-off) observations at 850 μm: 13.4 ± 2.1 mJy (Priddey et al. 2003b) and at 1200 μm: 5.5 ± 0.5 mJy (Petric et al. 2003). Submm emission is clearly visible in the maps (Fig. 1) at the optical coordinates of the quasar (the map centre), at both 850 μm (11.2 ± 1.0 mJy) and 450 μm (16 ± 5 mJy). To the eye, the source appears elongated; the best-fit 2-D Gaussian corresponds to (21.4 ± 9.0) arcsec × (13.6 ± 3.8) arcsec at a position angle (PA) of $69 \pm 37°$.

Three further sources were detected ($>3\sigma$) in the SDSS J0756+4104 field at 850 μm, each close the edge of the map (one beyond the areal coverage at 450 μm). In addition, two sources were detected at 450 μm, though neither has a robust 850-μm counterpart ($3\sigma < 4.5$ mJy). This casts some doubt on their reality; certainly, if they are real emitters, they are likely to be at a *much* lower redshift than the central quasar.

SDSS J1030+0524 (z = 6.28) has been the object of considerable observational study. Stiavelli et al. (2005), for example, detected two candidate $z \sim 6$ sources in *Hubble Space Telecope*

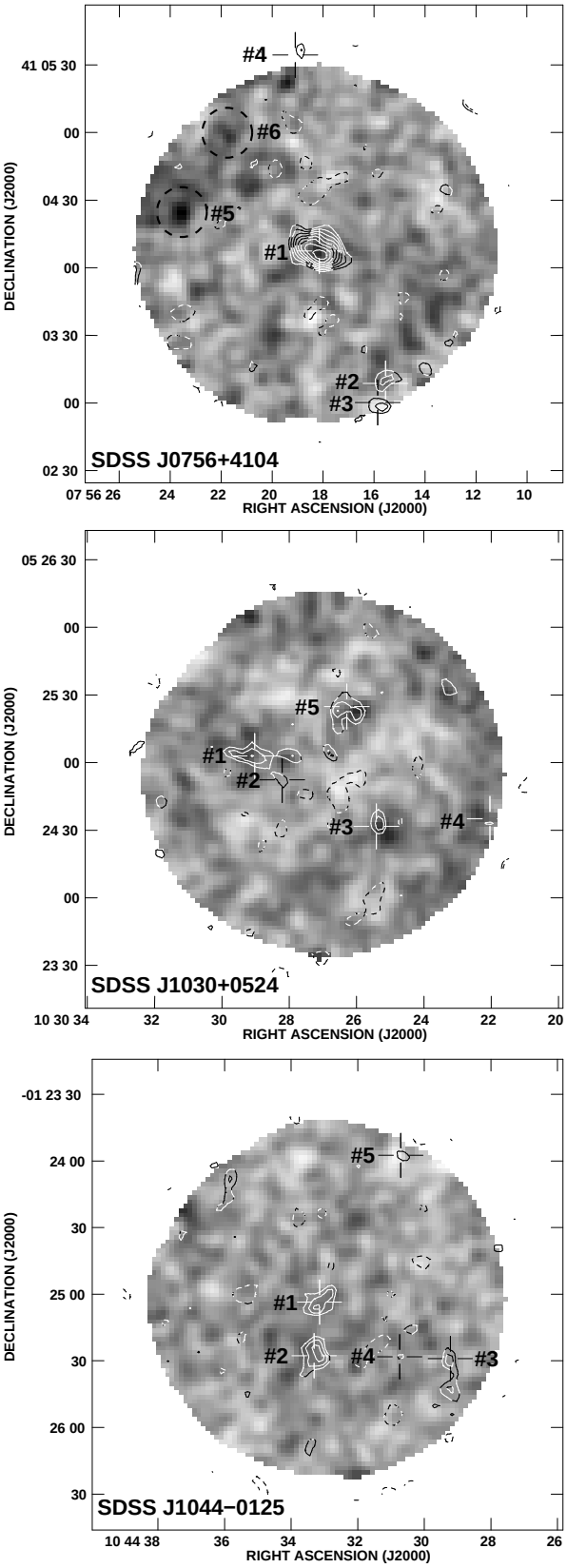

Figure 1. submm images of fields centred on three optically selected, radio-quiet quasars at $z > 5$. The 850-μm maps are plotted as contours, at levels -3, +3, 4, 5, 6... $\times\sigma$. The 450-μm images are displayed as greyscales. 850-μm sources (at $\geqslant 3\sigma$ significance) are identified with open crosses; their labels correspond to those in column 2 of Table 2. Sources detected only at 450 μm are circled.

Table 2. Properties of SMGs detected in quasar fields.

IAU Source Name	Id in Fig. 1	R.A. (J2000)	Dec. (J2000)	$S_{850\mu m}$ $\pm\sigma$ (mJy)†	S/N	$S_{450\mu m}$ $\pm\sigma$ (mJy)†
SDSS J0756+4104	#1	07 56 18.15	+41 04 07.5	13.4 ± 1.0	13.9	16 ± 5
SMM J075615.55+410308.7	#2	07 56 15.55	+41 03 08.7	4.4 ± 1.4	3.1	$3\sigma < 24$
SMM J075615.86+410300.2	#3	07 56 15.86	+41 03 00.2	4.6 ± 1.4	3.1	$3\sigma < 24$
SMM J075619.09+410534.4	#4	07 56 19.09	+41 05 34.4	13.1 ± 3.4	3.9	‡
SMM J075621.83+410459.9	#5	07 56 21.83	+41 04 59.9	$3\sigma < 5.1$	–	56 ± 13
SMM J075623.58+410424.6	#6	07 56 23.58	+41 04 24.6	$3\sigma < 5.1$	–	25 ± 8
SMM J103029.03+052502.9	#1	10 30 29.03	+05 25 02.9	7.5 ± 1.7	4.3	42 ± 12
SMM J103028.21+052452.3	#2	10 30 28.21	+05 24 52.3	5.3 ± 1.7	3.3	$3\sigma < 33$
SMM J103025.41+052431.7	#3	10 30 25.41	+05 24 31.7	6.8 ± 1.7	4.3	49 ± 11
SMM J103022.04+052435.0	#4	10 30 22.04	+05 24 35.0	7.0 ± 2.2	3.3	$3\sigma < 48$
SMM J103026.29+052524.9	#5	10 30 26.29	+05 25 24.9	8.5 ± 1.7	5.0	45 ± 10
SDSS J1044−0125	#1	10 44 33.15	−01 25 03.6	5.6 ± 1.0	6.2	$3\sigma < 24$
SMM J104433.31−012527.7	#2	10 44 33.31	−01 25 27.7	7.5 ± 1.5	5.5	24 ± 7
SMM J104429.22−012529.0	#3	10 44 29.22	−01 25 29.0	6.1 ± 1.7	3.5	$3\sigma < 24$
SMM J104430.74−012528.2	#4	10 44 30.74	−01 25 28.2	7.0 ± 1.7	4.5	$3\sigma < 24$
SMM J104430.71−012357.5	#5	10 44 30.71	−01 23 57.5	6.8 ± 1.9	3.0	‡

† Errors exclude the uncertainty in absolute flux calibration: 10 (25) per cent at 850 μm (450 μm).
‡ Outside region covered by 450-μm data.

(HST)–ACS images of the field, which they speculate may belong to the same dark matter halo. The quasar itself appears similar in all respects to low-redshift AGN: submm photometry failed to detect the quasar to a sensitive limit of $3\sigma < 3.0$ mJy at 850 μm (Priddey et al. 2003b) and a deep X-ray spectrum taken with *XMM-Newton* (Farrah et al. 2004) finds a photon index $\Gamma \approx 2.1$ with no evidence for intrinsic absorption ($N_{\rm H} < 8 \times 10^{22}$ cm^{-2}). The lack of gas and dust, plus the near-canonical X-ray spectral slope, suggest that this SMBH and its host have already passed through their major formation phase, only ∼900 Myr after the Big Bang.

Our submm images (Fig. 1) confirm the submm quiescence of the quasar/host galaxy, with 3-σ limits of 5.1 and 30 mJy at 850 and 450 μm, respectively. Indeed, there is an interesting negative feature just south-west of the quasar corresponding to the western "off" position of the weakest SMG in this field, probably the primary reason SMM J103028.21+052452.3 achieves an overall significance of $\geqslant 3\sigma$.

The surrounding field is crowded: five sources at 850 μm and three at 450 μm. Each of the 450-μm sources lies within a fraction of a beamwidth of significant 850-μm emission, confirming the reality of both.

Is it surprising that the least active quasar host should have the most active environment? It is possible that, by targeting luminous, *optically*-selected quasars, we are selecting very massive objects that are already close to the end of their star-forming phase. By the rules of "downsizing", the evolution of the most massive objects is completed earliest, so it should not be surprising to see companions to fully-formed, high-redshift quasars in an earlier evolutionary stage (see also Section 3.5).

A 1.4-GHz Very Large Array image ($\sigma \approx 20\,\mu$Jy) of the field was obtained by (Petric et al. 2003), comparison with which enables us to pinpoint counterparts at other wavelengths with sub-arcsec precision (e.g. Ivison et al. 1998). In addition, constraints can be placed on the redshifts of those sources with radio counterparts, or meaningful limits. SMM J103029.03+0452502.9 lies 6.8 arcsec from a radio source at $\alpha = 10^{\rm h}30^{\rm m}26.^{\rm s}0, \delta = +05^\circ25'19.''69$ with an integrated 1.4-GHz flux density of $427 \pm 52\,\mu$Jy (Andreea Petric, private communication), giving a spectral index, $\alpha_{1.4\rm GHz}^{350\rm GHz} = 0.52 \pm 0.04$. If the submm and radio sources are the same (and this is statistically very probable – $P < 0.05$ – see Ivison et al. 2002), the FIR–radio correlation for star-forming galaxies predicts $z = 1.0^{+0.7}_{-0.5}$ (Carilli & Yun 2000; see Figure 2). SMM J103025.41+052431.7 is near-coincident (separation, 4.4 arcsec) with the core of a limb-brightened Fanaroff–Riley II (FR II) radio galaxy (Fig. 2 of Petric et al.) – another statistically significant association, i.e. $P < 0.05$. This raises the strong suspicion, allied with their relatively high 450-μm flux densities, that some or all of the other nearby SMGs might lie in the foreground, associated with this radio galaxy, rather than at the redshift of the quasar. Such luminous radio galaxies are commonly found in clusters (Best et al. 2003, 2007) and some clusters are known to host SMGs (Best 2002; Webb et al. 2005).

SDSS J1044−0125 (z = 5.73) has an optical spectrum with a C IV absorption trough suggesting that this is a broad absorption line (BAL) quasar (Maiolino et al. 2001; Goodrich et al. 2001). Correspondingly, the quasar is weak in X-rays (Brandt et al. 2001), consistent with the BAL interpretation (e.g. Gallagher et al. 2006). The quasar/host was detected at 850 and 1200 μm using on-off measurements with SCUBA and MAMBO respectively: 6.1 ± 1.2 mJy and 2.5 ± 0.6 mJy (see Section 2.2).

In our SCUBA image, the quasar is detected robustly at 850 μm with a flux density of 5.7 ± 1.5 mJy, with weak evidence of extended emission (Section 3.4). Four further sources are detected at 850 μm; one at 450μm, corresponding to the brightest 850-μm emitter.

3 DISCUSSION AND ANALYSIS

3.1 Photometric redshifts

We can place crude constraints on the redshift of any 850-μm emitters in our quasar fields using detections or limits at 1.4 GHz and/or 450 μm. Much of the uncertainty in this procedure rests in the intrinsic diversity of SEDs exhibited by SMGs (Ivison et al. 2000b).

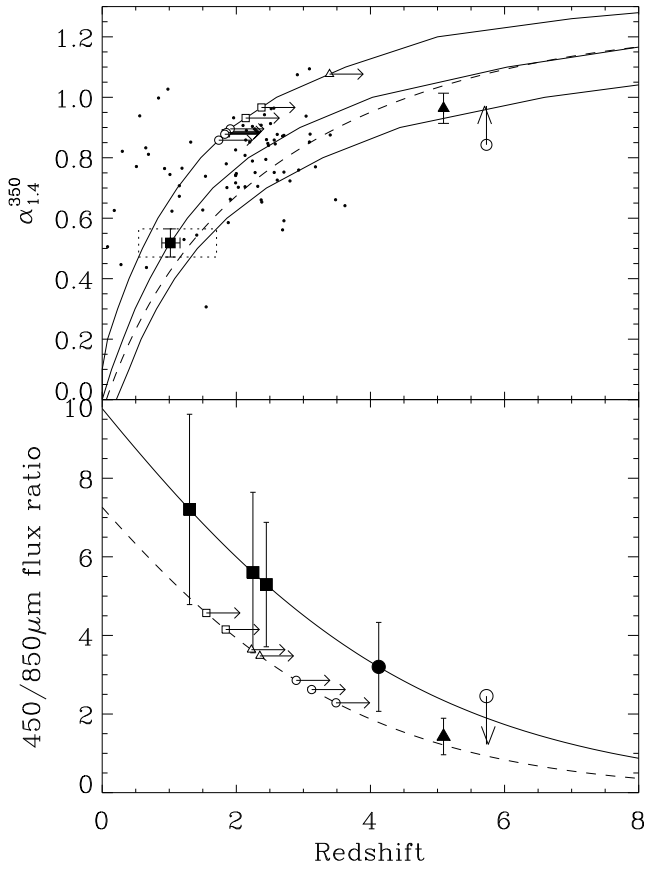

Figure 2. Top: submm (850 μm) to radio (1.4 GHz) spectral index as a redshift indicator. The curves show empirical calibrations from (thick solid, with $\pm1\sigma$ shown as thin solid) Carilli & Yun (2000) and (dashed) Yun & Carilli (2002). Also for comparison are plotted (small points) SMGs with spectroscopic redshifts and radio fluxes from Chapman et al. (2005). Sources in the SDSS J0756+4104 field are shown as triangles; in the SDSS J1030+0524 field, squares; in the SDSS J1044−0125 field, circles. Radio detections have filled symbols; upper limits are unfilled. Two of the quasars (SDSS J0756+4104 and SDSS J1044−0125) are plotted at their spectroscopic redshifts. A tentative radio counterpart to an SMG in the SDSS J1030+0524 field (#5) is shown with a dotted box delineating the 1σ uncertainty in its photometric redshift. Radio-undetected SMGs are plotted at the most conservative lower limit on their redshift, given by the upper curve from Carilli & Yun (2000). **Bottom:** 450 μm/850 μm ratio as a redshift indicator. The curves are derived from fits to the spectral energy distributions (SEDs) of $z > 4$ quasars (Priddey & McMahon 2001, solid) and SMGs (Coppin et al. 2007, dashed).

Radio imaging at 1.4 GHz of the three fields, reaching rms levels of 17, 20 and 27 μJy beam^{-1} for SDSS J0756+4104, SDSS J1030+0524 and SDSS J1044−0125, respectively, were published by Petric et al. (2003). As noted earlier, two sources in the SDSS J1030+0524 field have radio counterparts: identification of SMM J103026.29+052524.9 with a radio emitter implies $z \sim 1$, and SMM J103025.41+052431.7 is coincident with the core of a FR II radio galaxy. Of the two quasars with submm detections, SDSS J0756+4104 has a 1.4-GHz flux density of 65 ± 17 μJy, implying a spectral index, $\alpha_{1.4\mathrm{GHz}}^{350\mathrm{GHz}} = 0.93 \pm 0.05$; SDSS J1044−0125 has a radio upper limit, $3\sigma < 80$ μJy, giving $\alpha_{1.4\mathrm{GHz}}^{350\mathrm{GHz}} > 0.85$ (2σ). Both are consistent with starbursts, given their respective redshifts (Fig. 2). In Fig. 2 we also indicate the lower limits on $\alpha_{1.4\mathrm{GHz}}^{350\mathrm{GHz}}$ corresponding to SMGs *not* detected in the Petric et al. (2003) radio maps: all are consistent with the sources lying at high redshift, the weakest lower limits implying $z > 1.5$ (assuming a generous scatter in $\alpha_{1.4\mathrm{GHz}}^{350\mathrm{GHz}}$.)

Fig. 2 also illustrates the 450 μm/850 μm flux density ratio as a redshift indicator assuming idealised, isothermal, greybody dust spectra: one SED determined from $z > 4$ quasars by Priddey & McMahon (2001) with $T_\mathrm{d} = 42$ K, $\beta = 1.9$; another SED determined from blank-field SMGs in the SCUBA HAlf Degree Extragalactic Survey (SHADES) with $T_\mathrm{d} = 35$ K, $\beta = 1.5$ (Coppin et al. 2007). A low 450 μm/850 μm flux density ratio implies a high redshift since the observed 450-μm emission must have originated at the peak, or possibly on the Wien side, of the SED. Thus it is plausible that any 850-μm sources undetected in deep 450-μm data lie at high redshift, the most conservative constraints giving $z \gtrsim 2$. Conversely, a 450-μm emitter with no corresponding 850-μm detection can be considered to have a weak upper limit on its redshift.

Ideally, one would search for spectral features to establish the redshifts of the companion sources unambiguously. The rest-frame mid-IR, FIR and submm wavebands offer ionic/atomic fine-structure lines as well as the rotational transitions of molecular CO and HCN. Unfortunately, such observations are beyond the reach of current ground- and space-based instrumentation, though this will change with the advent of the Atacama Large Millimetre Array (ALMA) and future actively cooled space missions such as the Space Infrared Telescope for Cosmology and Astrophysics (SPICA – Nakagawa 2004) or the FIR Interferometer (FIRI – Helmich & Ivison 2007).

3.2 Number counts

Earlier submm/mm imaging surveys have shown evidence for overdensities of SMGs in the vicinities of AGN at high redshift: in fields around radio galaxies at $z \sim 4$ (e.g. Ivison et al. 2000a; Stevens et al. 2003; De Breuck et al. 2004; Greve et al. 2007) and in the field of an absorbed QSO at $z \sim 2$ (Stevens et al. 2004). Are our $z > 5$ QSO fields consistent with these findings?

Fig. 3 compares the cumulative number counts observed in our three $z > 5$ quasar fields ("z5Q") with (a) counts from Stevens et al. 2003 ("HzRG"); (b) blank-field submm survey counts (a fit to the SHADES counts by Coppin et al. 2006); (c) counts from submm imaging surveys of clusters at $z \sim 1$ (Best 2002; Webb et al. 2005). The raw number counts have been corrected for effective survey area as a function of limiting flux density. However, we have not corrected for incompleteness or for flux boosting. At the faintest levels, or in noisy regions of the map where sources lie near the flux limit, these effects are significant, but they are difficult to correct in maps of this size and involve assumptions about the number count distribution, e.g. using the blank-field counts with which we are attempting to compare.

Nevertheless, assuming Poisson errors there is a significant excess over the blank-field counts. The seven radio galaxy fields and the three z5Q fields each contain a total of 12 850-μm companion sources. The z5Q counts (and those of the $z \sim 1$ clusters) are consistent with the radio galaxy field counts (with the caveat that the z5Q sample spans a more limited range in flux density, due to shallower limit and smaller total area); both contain more SMGs than blank fields by a factor 4–5 across a range of 850-μm flux densities, including the $\gtrsim$6-mJy regime where the effects of flux boosting are minimal and overall sample reliability is excellent.

In a blank-field survey of equivalent area and depth to all three of our fields combined, one would expect (based upon model fits to

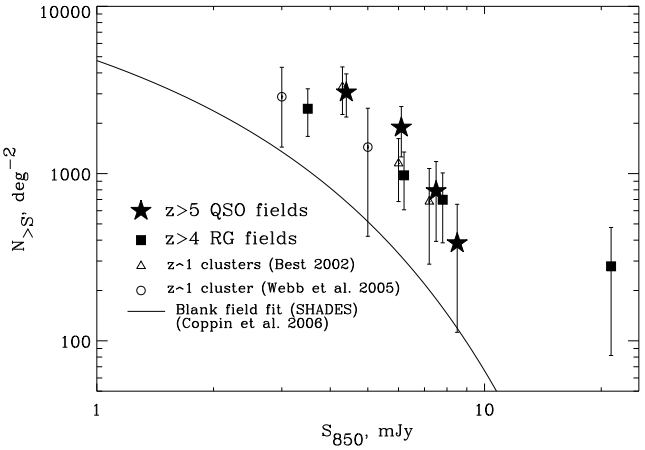

Figure 3. Cumulative number counts of SMGs, in fields centred on (i) luminous high-redshift AGN (filled symbols): $z > 5$ optically selected quasars (stars; this work); $z \sim 4$ radio galaxies (squares; Stevens et al. 2003); and (ii) $z \sim 1$ clusters (unfilled symbols – Best 2002; Webb et al. 2005). The line shows a functional fit to the blank-field number counts of SMGs in the SHADES submm survey (Coppin et al. 2006). Points have been corrected for effective area as a function of survey depth, but not for flux boosting, confusion or incompleteness. Even so, the excess over the blank-field counts is striking.

the SHADES counts from Coppin et al. 2006) to detect ∼3, ∼2 and ∼1 sources brighter than $S_{850\mu\mathrm{m}}$ = 4.1, 5.4 and 7.3 mJy, respectively. It is thus likely that some of the 12 z5Q companion sources are foreground contaminants, as we have seen already in §3.1. Others, as we have also seen, are consistent with SMGs at high redshift, based on their radio/submm and 450 μm/850 μm flux density ratios. We conclude that the maps probably contain SMGs genuinely associated with the dark matter haloes inhabited by our target quasars, leading to the statistical overdensities observed.

As well as the potential for foreground objects to contaminate the sample directly via their submm emission, we should consider whether the observed excess of SMGs may be due to their gravitational lensing effects (e.g. Chapman et al. 2002). Depending on the slope of the luminosity function, Wyithe & Loeb (2002) estimate that $\sim \frac{1}{14} - \frac{1}{3}$ of $z \sim 6$ quasars could be lensed. Targeting two submm-bright quasar hosts may have introduced an additional bias toward lensed fields, while the possibility that the submm-faint host is lensed is enhanced by the presence of a foreground radio galaxy (and possibly a cluster associated with that radio galaxy). The degree to which number counts are boosted by lensing depends on a competition between (i) the abundance of faint sources available to be boosted by the gravitational magnification and (ii) the stretching of area in the source plane. Since the submm source counts are steep, (i) is a strong effect. Deep optical images of $z > 5$ quasars, including SDSS J1030+0524, have failed to reveal any morphological signatures of strong lensing (Fan et al. 2003). Neither are line-of-sight galaxies, that could provide magnifications greater than ∼1.1, in evidence (Willott et al. 2005). For now, therefore, we consider the observed overdensity to be due to high-redshift SMGs in the vicinity of the signpost quasars, rather than lensing or unusual foreground activity.

3.3 Star-formation rates and dust masses at $z > 5$

We can estimate SFRs for SMGs from their 850-μm flux densities, $S_{850\mu\mathrm{m}}$, assuming that they lie at the redshifts of the quasars. The range of FIR luminosity of a source at the average redshift of the three quasars ($z = 5.7$) is L_{FIR} = 0.7→1.4 $\times(S_{850\mu\mathrm{m}}/\mathrm{mJy}) \times 10^{12}\,\mathrm{L}_\odot$, assuming thermal SEDs with T_d = 35–42 K and β = 1.5–1.9. If L_{FIR} is powered by reprocessed stellar light, this translates into an instantaneous formation rate of massive stars of $\Psi \times (L_{\mathrm{FIR}}/10^{10}\mathrm{L}_\odot)\,\mathrm{M}_\odot\,\mathrm{yr}^{-1}$. Here, Ψ depends upon factors such as the stellar mass function and the efficiency with which starlight is reprocessed by dust; we assume $\Psi \sim 1$ giving a SFR range of 70→140 $\times(S_{850\mu\mathrm{m}}/\mathrm{mJy})\,\mathrm{M}_\odot\,\mathrm{yr}^{-1}$. Summing up the contributions of the companion SMGs (but not of the quasars, to avoid AGN contamination, even though it is likely that a substantial fraction of their submm luminosity is due to star formation) gives a total SFR per field, averaged over the three maps, of $\approx f_{z>5}\times$ 2000→4000 $\mathrm{M}_\odot\,\mathrm{yr}^{-1}$, where $f_{z>5}$ represents the fraction of sources at the quasar redshifts. This star formation is apparently taking place in a region of volume $\lesssim$1 Mpc^3.

Adopting a dust opacity $\kappa_{125\mu\mathrm{m}} = 30\,\mathrm{cm}^2\,\mathrm{g}^{-1}$ (see Priddey et al. 2003b for an explanation), the dust mass corresponding to $S_{850\mu\mathrm{m}}$ is M_d = 0.5→1.0 $\times(S_{850\mu\mathrm{m}}/\mathrm{mJy}) \times 10^8\,\mathrm{M}_\odot$, giving a total dust mass per field of $\approx f_{z>5}\times$ 1.6→2.8 $\times 10^9\,\mathrm{M}_\odot$. In this case it is valid to include the quasar contribution, regardless of whether their submm luminosity is powered by starburst or AGN. The result is ∼1.9→3.3 $\times 10^9\,\mathrm{M}_\odot$). If the dust-to-gas ratio in these objects is similar to that of the Milky Way, their total gas mass is $\sim (S_{850\mu\mathrm{m}}/\mathrm{mJy}) \times 10^{10}\,\mathrm{M}_\odot$.

Finally, we consider the possibility that some of the submm companions are powered by buried AGN rather than obscured star formation. This is not implausible given evolutionary scenarios for SMGs involving co-evolution between black holes and massive spheroids. Assuming, in the most extreme case, that L_{FIR} represents the bolometric luminosity of the AGN, and assuming Eddington-limited accretion, the brightest SMGs (≈10 mJy) would have black holes of mass $\approx 4 \times 10^8\,\mathrm{M}_\odot$. Their hard X-ray fluxes (2–10 keV) would be $\approx 4 \times 10^{-15}\,\mathrm{erg\,cm^{-2}\,s^{-1}}$. For the general SMG population, or at least the radio-identified subset, deep X-ray observations (e.g. Alexander et al. 2005) show that their AGN are weak compared with their bolometric luminosity. We have no reason to believe the SMGs in our high-redshift quasar fields should be any different; indeed, their SMBHs are likely somewhat less developed than those explored by Alexander et al. at $z \sim 2.2$.

3.4 Resolved emission and radial profiles

To measure source sizes requires knowledge of the PSF, determined to be 13.4 arcsec FWHM and near-circular by fitting a 2-dimensional (2-D) Gaussian to a beam map of 3C 345. We have used these parameters to determine the size of the most significant ($> 6\sigma$) sources, again using 2-D Gaussian fits within the AIPS software environment.

SDSS J0756+4104 appears to be resolved along an axis with PA 69°. Along the orthogonal axis, the quasar's submm emission is point-like. Deconvolving the beam from the best-bet 2-D Gaussian fit suggests an emission region of size (16.0 ± 1.5) arcsec $\times$ (0.0 ± 1.5) arcsec, though the apparent morphology could be mimicked by two or more well-separated, compact sources.

At first sight SDSS J1044−0125 also appears resolved, albeit with less certainty than for the $\sim 14\sigma$ detection of SDSS J0756+4104. However, the best-fit 2-D Gaussian has dimensions similar to those of the beam: (14.4 ± 2.5) arcsec $\times$ (12.5 ± 2.5) arcsec at PA 125°, so we conclude that there is no compelling evidence that the emission from SDSS J1044−0125 has been resolved.

The angular scale is ≈6 kpc arcsec^{-1} at $z \sim 5-6$, so the physical scale of the emission from SDSS J0756+4104 corresponds to ≈100 kpc on the plane of the sky. This suggests, perhaps, that we are witnessing a colossal merger. Lensing might provide an alternative explanation, though there is scant evidence for this from optical images.

Evidence of source structure deviating from that of a point source has been noted in previous submm observations of high-redshift galaxies (e.g. Ivison et al. 2000a; Stevens et al. 2003). The mm continuum and CO line emission from the $z = 4.7$ quasar, BR 1202−0725, was clearly separated into two components by Omont et al. (1996), albeit with a smaller angular separation (4 arcsec) than single-dish submm imaging is capable of resolving. Several high-redshift radio galaxies have also been resolved in CO line emission (Papadopoulos et al. 2000; De Breuck et al. 2005) on arcsec scales using the IRAM Plateau de Bure interferometer (PdBI).

3.5 Comparison with model predictions

The linear Press–Schechter approximation can be used to demonstrate analytically the concept of bias in a hierarchical cosmology (e.g. Mo & White 2002). However, numerical simulations of the evolution of CDM, which can track the collapse of fluctuations on large scales into the non-linear regime, reveal a more complex picture, the dark matter exhibiting a rich spatial structure (filaments, clusters: the so-called "cosmic web").

In the "Millenium Simulation", Springel et al. (2005) specifically identify $z = 6$ quasars, selecting them as the objects with the most massive dark matter haloes and/or the largest stellar mass. These objects have halo masses $\sim 10^{12.5}\,M_\odot$, SFRs of several $100\,M_\odot\,yr^{-1}$ and evolve into the central dominant galaxies of rich clusters at $z = 0$. At $z = 6$ they are surrounded by numerous star-forming galaxies and lie on prominent dark matter filaments (Fig. 3 of Springel et al. 2005). The knots strung out on these filaments are reminiscent of the submm companions to $z > 5$ quasars – especially, for example, the neighbouring pair in the SDSS J0756+4104 image (Fig. 1), and the possible binarity of the quasar host itself. However, such claims are premature: the angular scale over which one would confidently expect to see large-scale structure is somewhat greater than that enclosed within the field-of-view of SCUBA. The present images correspond only to the innermost ∼1 Mpc of such structures.

A tentative evolutionary scheme in which to interpret our observations is the "anti-hierarchical" model of Granato et al. (2004, 2006). This scheme not only incorporates the effects of feedback from the AGN on star formation, but explicitly takes account of dust. A counter-intuitive feature of this model is that the evolution progresses more rapidly for the most massive objects. SMGs are envisaged as massive spheroids undergoing a major episode of dust-enshrouded star formation, containing small (but gradually accreting) black holes in their cores. Eventually the black hole becomes sufficiently massive to power a quasar, thereby terminating star formation via jets in radio-loud systems or via accretion-driven winds in radio-quiet objects. The system then evolves passively as a massive elliptical galaxy to the present day. Submm-luminous high-redshift quasars presumably correspond to the late stages of this transition between SMG and QSO (Page et al. 2004; Stevens et al. 2005). If the QSO represents the most massive collapsed object in its field (by design we have selected extremely luminous objects), it will have a head start over the SMGs in its field. As suggested earlier, it may not be surprising that SDSS J1030+0524 is "submm dead", despite residing in the most active field: it may have evolved more rapidly than its companions and expended its fuel.

4 SUMMARY

Submm images at 450 and 850 μm of the fields of optically luminous $z > 5$ quasars reveal an excess of submm emitters relative to expected counts of SMGs in blank fields. Although flux ratios show that some of the companion SMGs are undoubtedly foreground objects, the submm counts suggest that many of these companions probably lie in the dark matter haloes inhabited by our target quasars

Two of the quasars are luminous submm emitters in their own right, suggesting that their hosts are intensely star-forming galaxies. Furthermore, one shows tentative signs of extended submm emission, an indication either that the host galaxy is resolved (on a ∼100-kpc scale) or, more likely, is caught during a merger. This finding reinforces, and extends to higher redshift, the conclusions of previous submm/mm imaging surveys of high-redshift AGN.

The observed overdensities of luminous, star-forming galaxies are consistent with the idea that luminous AGN reside in the most massive dark matter haloes at any epoch and, as such, pinpoint highly biased regions in the high-redshift Universe which eventually merge to become rich clusters in the present day. Any more detailed interpretation is hindered by the limitations of present instrumentation but forthcoming FIR and submm facilities will enable significant progress to be made.

- At current sensitivity levels, set by confusion at ∼2 mJy at 850 μm, we are sensitive only to the very brightest starbursts – several $\times 100\,M_\odot\,yr^{-1}$ of star formation, not at all typical of known $z > 5$ field galaxies. However in the future, facilities such as ALMA will provide a powerful means of locating more typical star-forming galaxies at high redshift. It is important to characterise the feasibility of such a project by learning what we can about the role of dust in the formation of the earliest galaxies. The presence of dust at these redshifts may have significant implications for reionization, as well as for Lyman-α line searches for high-redshift galaxies – the escape into the intergalactic medium of UV photons being hindered and thermally degraded by dust grains.
- The large beam size of the JCMT at 850μm precludes scrutiny of the sources on fine spatial scales, yet provides a tantalising glimpse of partially resolved or interacting galaxies. The enhanced resolution of submm interferometers such as IRAM PdBI and, ultimately, ALMA, will allow for more intricate study of the morphology and dynamics of high-redshift starbursts.
- The high areal mapping speed offered by SCUBA-2 (Holland et al. 2006) opens up the possibility that we will be able to trace the distribution of star-forming galaxies on wide scales surrounding luminous, high-redshift AGN, obtaining surer statistics, perhaps even tracing the dark matter filaments and thus directly testing some of the predictions of numerical simulations of CDM models.
- Wide-field spectral imaging at mid-IR–mm wavelengths offers the best prospects with which to determine the redshifts of SMGs in the quasar fields unambiguously. Whilst such observations are beyond the capabilities of current facilities, the sensitivities of ALMA and future FIR space missions will be sufficient to pinpoint dusty, star-forming galaxies out to $z \sim 6$.

The prospects implied by these discoveries for the next generation of submm instruments are therefore extremely promising.

ACKNOWLEDGEMENTS

RSP gratefully acknowledges support from the University of Hertfordshire. The JCMT is operated on behalf of the UK Science and Technology Facilities Council, the Netherlands Organisation for Scientific Research and the National Research Council of Canada.

References

Alexander D. M., Bauer F. E., Chapman S. C., Smail I., Blain A. W., Brandt W. N., Ivison R. J., 2005, ApJ, 632, 736
Anderson S. F. et al., 2001, AJ, 122, 503
Becker R. H. et al., 2001, AJ, 122, 2850
Best P. N., 2002, MNRAS, 336, 1293
Best P. N., Lehnert M. D., Miley G. K., Röttgering H. J. A., 2003, MNRAS, 343, 1
Best P. N., von der Linden A., Kauffmann G., Heckman T. M., Kaiser C. R., 2007, MNRAS, 527
Bouwens R. J., Illingworth G. D., Blakeslee J. P., Franx M., 2006, ApJ, 653, 53
Brandt W. N., Guainazzi M., Kaspi S., Fan X., Schneider D. P., Strauss M. A., Clavel J., Gunn J. E., 2001, AJ, 121, 591
Bunker A. J., Stanway E. R., Ellis R. S., McMahon R. G., 2004, MNRAS, 355, 374
Carilli C. L., Yun M. S., 2000, ApJ, 530, 618
Chapman S. C., Blain A. W., Smail I., Ivison R. J., 2005, ApJ, 622, 772
Chapman S. C., Smail I., Ivison R. J., Blain A. W., 2002, MNRAS, 335, L17
Coppin K. et al., 2006, MNRAS, 372, 1621
Coppin K. et al., 2007, MNRAS, submitted
Croom S. M. et al., 2005, MNRAS, 356, 415
De Breuck C. et al., 2004, A&A, 424, 1
De Breuck C., Downes D., Neri R., van Breugel W., Reuland M., Omont A., Ivison R., 2005, A&A, 430, L1
Efstathiou G., Rees M. J., 1988, MNRAS, 230, 5P
Elvis M. et al., 1994, ApJS, 95, 1
Fan X., Carilli C. L., Keating B., 2006, ARA&A, 44, 415
Fan X. et al., 2001, AJ, 122, 2833
Fan X. et al., 2006, AJ, 131, 1203
Fan X. et al., 2003, AJ, 125, 1649
Fan X. et al., 2000, AJ, 120, 1167
Farrah D., Priddey R., Wilman R., Haehnelt M., McMahon R., 2004, ApJ, 611, L13
Gallagher S. C., Brandt W. N., Chartas G., Priddey R., Garmire G. P., Sambruna R. M., 2006, ApJ, 644, 709
Goodrich R. W. et al., 2001, ApJ, 561, L23
Granato G. L., De Zotti G., Silva L., Bressan A., Danese L., 2004, ApJ, 600, 580
Granato G. L., Silva L., Lapi A., Shankar F., De Zotti G., Danese L., 2006, MNRAS, 368, L72
Greve T. R., Stern D., Ivison R. J., De Breuck C., Kovács A., Bertoldi F., 2007, ArXiv e-prints, 707
Gunn J. E., Peterson B. A., 1965, ApJ, 142, 1633
Haislip J. B. et al., 2006, Nature, 440, 181
Helmich F., Ivison R., 2007, ArXiv e-prints, 707
Holland W. et al., 2006, in SPIE, Vol. 6275, Millimeter and Submillimeter Detectors and Instrumentation for Astronomy III. eds Zmuidzinas J. et al., p. 6275
Holland W. S. et al., 1999, MNRAS, 303, 659
Isaak K. G., Priddey R. S., McMahon R. G., Omont A., Péroux C., Sharp R. G., Withington S., 2002, MNRAS, 329, 149
Ivison R. J., 2006, MNRAS, 370, 495
Ivison R. J., Dunlop J. S., Smail I., Dey A., Liu M. C., Graham J. R., 2000a, ApJ, 542, 27
Ivison R. J. et al., 2002, MNRAS, 337, 1
Ivison R. J., Smail I., Barger A. J., Kneib J.-P., Blain A. W., Owen F. N., Kerr T. H., Cowie L. L., 2000b, MNRAS, 315, 209
Ivison R. J., Smail I., Le Borgne J.-F., Blain A. W., Kneib J.-P., Bezecourt J., Kerr T. H., Davies J. K., 1998, MNRAS, 298, 583
Jakobsson P. et al., 2006, A&A, 447, 897
Jenness T., Lightfoot J. F., 1998, in Albrecht R., Hook R., Bushouse H., ed, Astronomical Data Analysis Software and Systems VII., A.S.P. Conference Series, Vol. 145, p. 216
Kaiser N., 1984, ApJ, 284, L9
Maiolino R., Mannucci F., Baffa C., Gennari S., Oliva E., 2001, A&A, 372, L5
Mo H. J., White S. D. M., 2002, MNRAS, 336, 112
Nakagawa T., 2004, Advances in Space Research, 34, 645
Omont A., Petitjean P., Guilloteau S., McMahon R. G., Solomon P. M., Pécontal E., 1996, Nature, 382, 428
Page M. J., Stevens J. A., Ivison R. J., Carrera F. J., 2004, ApJ, 611, L85
Papadopoulos P. P., Röttgering H. J. A., van der Werf P. P., Guilloteau S., Omont A., van Breugel W. J. M., Tilanus R. P. J., 2000, ApJ, 528, 626
Petric A. O., Carilli C. L., Bertoldi F., Fan X., Cox P., Strauss M. A., Omont A., Schneider D. P., 2003, AJ, 126, 15
Priddey R. S., Isaak K. G., McMahon R. G., Omont A., 2003a, MNRAS, 339, 1183
Priddey R. S., Isaak K. G., McMahon R. G., Robson E. I., Pearson C. P., 2003b, MNRAS, 344, L74
Priddey R. S., McMahon R. G., 2001, MNRAS, 324, L17
Robson I., Priddey R. S., Isaak K. G., McMahon R. G., 2004, MNRAS, 351, L29
Scott S. E. et al., 2002, MNRAS, 331, 817
Spergel D. N. et al., 2007, ApJS, 170, 377
Springel V. et al., 2005, Nature, 435, 629
Srbinovsky J. A., Wyithe J. S. B., 2007, MNRAS, 374, 627
Stevens J. A. et al., 2003, Nature, 425, 264
Stevens J. A., Page M. J., Ivison R. J., Carrera F. J., Mittaz J. P. D., Smail I., McHardy I. M., 2005, MNRAS, 360, 610
Stevens J. A., Page M. J., Ivison R. J., Smail I., Carrera F. J., 2004, ApJ, 604, L17
Stiavelli M. et al., 2005, ApJ, 622, L1
Walter F. et al., 2003, Nature, 424, 406
Walter F., Carilli C., Bertoldi F., Menten K., Cox P., Lo K. Y., Fan X., Strauss M. A., 2004, ApJ, 615, L17
Webb T. M. A., Yee H. K. C., Ivison R. J., Hoekstra H., Gladders M. D., Barrientos L. F., Hsieh B. C., 2005, ApJ, 631, 187
Willott C. J., McLure R. J., Jarvis M. J., 2003, ApJ, 587, L15
Willott C. J., Percival W. J., McLure R. J., Crampton D., Hutchings J. B., Jarvis M. J., Sawicki M., Simard L., 2005, ApJ, 626, 657
Wyithe J. S. B., Loeb A., 2002, ApJ, 577, 57
Yun M. S., Carilli C. L., 2002, ApJ, 568, 88